Autophagy modulation in primary culture of porcine satellite cells

Annie Vincent, Isabelle Louveau, Frédéric Dessauge

animal - open space 2 (2023) 100042

Contents lists available at ScienceDirect

animal - open space

Method paper

Autophagy modulation in primary culture of porcine satellite cells

A. Vincent, I. Louveau, F. Dessauge *

PEGASE, INRAE, Institut Agro, 35590 Saint-Gilles, France

ARTICLE INFO

Article history:
Received 22 November 2022
Revised 15 March 2023
Accepted 23 March 2023

Handling editor: Carlotta Giromini

Keywords:
Autophagosome
Metabolism
Muscle
Myotubes
Pig

ABSTRACT

Autophagy is a lysosomal degradation pathway with a role in the turnover of cell components via self-digestion. Over the past decade, it has been recognised as an essential process to maintain cellular and energy homeostasis. Nevertheless, little attention has been paid to this process in farm animals. In pigs, the role of autophagy in skeletal muscle homeostasis and more specifically on the formation of multinucleated muscle fibres needs to be determined. Primary culture of satellite cells, the resident muscle stem cells, is an appropriate model to investigate macroautophagy (hereafter autophagy), the main autophagy process. The objective of the current study was to evaluate tools to monitor autophagy in this cell model and to specify the role of autophagy on cell differentiation. Samples of *longissimus* muscle were collected from 3- to 4-day-old piglets. After isolation, satellite cells were plated in growth medium, allowed to proliferate up to 80% confluence and then placed in an appropriate culture medium to differentiate into myotubes. Cells were explored from day 0 to day 3 of differentiation. Autophagy-related proteins and Adenosine Mono Phosphate-activated protein kinase (**AMPK**), a major sensor for cell energy, were detected by Western blotting. Expression of genes related to autophagy were also quantified by qPCR. The Microtubule-associated protein 1 light-chain 3β forms ratio increased during cell differentiation whereas phosphatidylinositol 3-kinase and sequestosome 1 proteins decreased significantly. Mitochondrial protein expression also decreased significantly with satellite cell differentiation. Then, cell treatment with an inhibitor of autophagy flux, Bafilomycin A1, confirmed that autophagy was activated during the conversion of myoblasts into myotubes along with AMPK activation in our satellite cell culture model. In conclusion, we provided tools for porcine autophagy investigation in tissues or cells and demonstrated that basal autophagy and energy metabolism are concomitantly modulated during porcine myogenesis *in vitro*.

Reader comments

We invite you to comment on the article on the PubPeer platform by clicking on this link discuss this article.

Implications

Autophagy has come up as an essential process in cellular maintenance and development in skeletal muscle, an important tissue for pig production. The present study was undertaken to identify molecular tools to monitor autophagy in pigs. Our study validated molecular markers that will be useful to investigate muscle growth and to further study autophagy signalling pathways in multiple cell types and organs in pigs.

Specification table

Subject	Physiology and Functional Biology
Type of data	Data were obtained from a study in which porcine satellite cells were cultured. After protein and RNA extractions, western blots and qPCR were performed to quantify proteins and mRNA levels in cultured cells.
How data were acquired	Microscope (Axio Imager M2, Zeiss) and ImageJ software, Camera system (ImageQuant LAS4000, GE Healthcare) and ImageQuant TL software, qPCR system (StepOnePlus, Thermo Fischer Scientific)

(*continued on next page*)

* Corresponding author.
E-mail address: frederic.dessauge@inrae.fr (F. Dessauge).

https://doi.org/10.1016/j.anopes.2023.100042

	R software for statistical analyses
Data format	Processed and calculated data in Excel and reported results as figures.
Parameters for data collection	Three crossbred female piglets (Piétrain x (Large White x Landrace) raised in standard conditions from the INRAE UE3P experimental facility (Saint-Gilles, France; https://doi.org/10.15454/1.5573932732039927E12) were killed at 3 or 4 days of age (1.94 ± 0.10 kg) and samples (15–20 g) of *longissimus* muscle were collected to isolate satellite cells and to culture cells subsequently *in vitro*.
Description of data collection	The fusion percentage of cultured satellite cells was estimated by fluorescence microscopy using ImageJ software (Schneider et al., 2012) from four randomly chosen fields per animal. For proteins, intensities of Western blot bands were quantified using ImageQuant LAS4000 (GE Healthcare) with ImageQuant TL software. Gene expression was quantified by qPCR and generated raw data were analyzed with Step One Plus software v2.3 (Thermo Fischer Scientific).
Data source location	Institution: INRAE City/Town/Region: Saint-Gilles Country: France Latitude and longitude: 48°8′37.332″N, 1°49′56.595″; GPS coordinates: 48.1452, −1.830114
Data accessibility	Repository name: Recherche data gouv Data identification number: https://doi.org/10.57745/F0XZP8
Related research article	No research article is related to this article.

Introduction

Skeletal muscle is made up of multinucleated myofibres, mainly formed during prenatal development, in which there are resident mesenchymal stem cells: the satellite cells (Biressi et al., 2007; Danoviz and Yablonka-Reuveni, 2012). These cells have the capacity to fuse with myofibres generating new myonuclei during growth and to regenerate muscle following injury or stress (Cheung and Rando, 2013; Montarras et al., 2013). Under physiological conditions, satellite cells remain quiescent and exhibit low transcriptional activity as well as low metabolism (Relaix et al., 2021). The activation of satellite cells when they fuse into multinucleated myofibres is closely associated with a metabolic reprogramming of the cellular metabolism and mitochondrial network (Fortini et al., 2016; Sin et al., 2016).

Recent advances highlighted autophagy as a very important intracellular mechanism that degrades cytosolic proteins and organelles to maintain cellular homeostasis. Macroautophagy, referred here to autophagy, is a multistep process involving several sequential steps: formation of a sequestering compartment, fusion with the lysosome, degradation and utilisation of the degraded products (Mizushima; 2007). Its role in pathological and physiological conditions has been reported during the past decade, and it is now well established that it plays an important role in tissue development especially in muscle (Masiero et al., 2009; Tang and Rando, 2014; Zecchini et al., 2018; Perrotta et al., 2020). Few studies have been devoted to its role in metabolism and growth in farm animals (Tesseraud et al., 2021). Moreover, the impact of this cellular process on pig muscle development has been mostly highlighted in response to nutrition in piglets or growing pigs (Suryawan and Davis, 2014; Rubio-González et al., 2015). In contrast, the contribution of autophagy in the activation and differentiation of satellite cells has been poorly studied, particularly in pigs. The current study was undertaken to enrich our preliminary studies (Vincent et al., 2020) and further identify other molecular tools that will be useful to investigate more extensively the role of autophagy during myogenic differentiation in piglets and more generally in the physiology of pigs.

Material and methods

Animal and muscle sampling

The experiment was performed in the INRAE UE3P experimental facility (Saint-Gilles, France; (https://doi.org/10.15454/1.5573932732039927E12) in compliance with the ethical standards of the European Community (Directive 2010/63/EU). Crossbred female pigs (Piétrain × (Large White × Landrace); n = 3) were slaughtered by electrical stunning and exsanguination at 3 or 4 days of age. Muscle samples (15–20 g) were aseptically collected from *longissimus* muscle (**LM**), a predominant fast-twitch glycolytic muscle involved in voluntary movements of the back, and placed on ice in 20 mL Dulbecco's Phosphate Buffer Saline (**DPBS**; Dutscher, Bernolsheim, France) containing 1% glucose (Sigma Aldrich, Saint-Quentin-Fallavier, France).

Satellite cell isolation

Satellite cells (**SCs**) were isolated from LM as previously described (Theil et al., 2006; Perruchot et al., 2012). Briefly, connective tissue was removed from muscle samples, finely cut with scissors on Petri dishes in a minimal quantity of DPBS buffer and digested 20 min in a shaking water bath at 37 °C in isolation medium containing 1.5 mg/mL collagenase-type II (Worthington biochemical, Lakewood, USA), 0.25% trypsin (Dutscher) and 0.01% DNase (Sigma Aldrich). The digestion was stopped by being on ice for 5 min, and the supernatant was removed and diluted 1:1 with growth medium (**GM**), (DMEM Glutamax, Fischer Scientific, Illkirch, France) supplemented with penicillin/streptomycin 500 UI/mL (Fischer Scientific), 10% Horse Serum (Fischer Scientific) and 10% Foetal Bovine Serum (Fischer Scientific). The remaining solution was replenished with isolation medium, and the procedure was repeated twice. Cell suspensions from successive digestion were pooled, centrifuged at 800*g* for 10 min at 4 °C, gently resuspended with GM and filtered through 200 µm and 50 µm Nytex filter. Filtered cells were centrifuged twice at 800*g* for 10 min at 4 °C and finally resuspended in 2 × 5 mL GM. Then, cells were centrifuged on top of a 20% Percoll gradient at 15 000*g* for 8 min at 4 °C to enrich the population in satellite cells. The lower part in centrifugation tube was collected in ice cold GM, centrifuged at 800*g* for 10 min at 4 °C and finally resuspended in 5 mL cold GM. Cell number was quantified using TC20 automated cell counter with Trypan blue (Bio-Rad, Marnes-la-Coquette, France). The average number of alive satellite cells was approximately 10^6 cells per gram of fresh muscle.

Satellite cell culture and autophagy flux assays

Isolated satellite cells were seeded at a density of 70 000 viable cells/cm^2 in six-well plates (9.6 cm^2/well) coated with Matrigel (1/50 v/v, Fischer Scientific) and grown in GM at 37 °C under 5% CO_2. Cells proliferated up to 80% confluence and were placed in Transition Medium (TM) (DMEM Glutamax supplemented with penicillin/streptomycin 500 UI/mL, 10% Foetal Bovine Serum) during 24 h. Finally, cells were placed in Differentiation Medium (**DM**; DMEM Glutamax supplemented with penicillin/streptomycin 500 UI/mL, 5% Foetal Bovine Serum, 1 μM porcine insulin (Sigma Aldrich) and 1 μM cytosine arabinoside (Sigma Aldrich)) up to 3 days.

To assess autophagy flux, cells were treated with 100 nM bafilomycin A1 (BioViotica, Liestal, Switzerland), or equivalent Dimethyl Sulfoxide (**DMSO**) for control treatment, diluted in medium, for 2 h prior to trypsinisation at confluence (**D0**), 1 day (**D1**) and 3 days (**D3**) after differentiation induction. Cells were rinsed three times in DPBS buffer, centrifuged at 800*g* for 10 min at 4 °C and dry pellets were stored at −80 °C before Western blot and qPCR analyses.

Immunofluorescence staining

For myosin heavy chain (**MyHC**) immunocytochemical detection, cells were fixed in ethanol at −20 °C for 15 min and washed with DPBS. Cells were then permeabilised in DPBS with 0.1% Triton for 10 min at ambient temperature. Cells were washed and blocked in DPBS with 0.5% bovine serum albumin (**BSA**). Cells were incubated with MF20 primary antibody (1:10, DSHB, Iowa City, USA) diluted in DPBS with 0.5% BSA at 37 °C for 2 h. Cells were washed, incubated in fluorescent secondary antibody (1: 1 000, A-21202, Fischer Scientific) for 1 h in the dark at room temperature, washed again and finally mounted in medium containing 4,6-diamidino-2-phenylindole (**DAPI**) (Fischer Scientific). Images were captured with Zeiss Axio Imager M2 microscope (Zeiss, Marly-Le-Roi, France). The fusion percentage was estimated using ImageJ software (Schneider et al., 2012) from four randomly chosen fields per animal corresponding to a total of 800–1 800 nuclei and expressed as the number of DAPI-stained nuclei inside myotubes divided by the total number of nuclei.

Western blot analyses

Whole-cell homogenates (20 μg of proteins) were separated by sodium dodecyl sulphate-polyacrylamide gel electrophoresis, electro-transferred to polyvinylidene difluoride membranes and incubated overnight at 4 °C with corresponding primary antibodies as described previously (Faure et al., 2013). Detailed information on antibodies is provided in Table 1. After five washes in Tris-buffered saline (**TBS**)-0.1%Tween, membranes were incubated with the appropriate horseradish peroxidase-conjugated secondary antibodies for 1 h at room temperature. After five washes in TBS-0.1% Tween, blots were developed by using an enhanced chemiluminescence kit (GE Healthcare Sciences), scanned with an ImageQuant LAS 4 000 system (GE Healthcare) and analysed with the ImageQuant TL program. For normalisation of each target protein expression, the band intensity of each sample was divided by the band intensity of a reference sample added on each gel (n = 3 gels). This reference sample was obtained by pooling all samples. The final normalised band intensity of each target protein was expressed as arbitrary units.

Quantitative PCR analyses

Total RNAs were extracted using a commercial kit (NucleoSpin RNA XS kit, Macherey-Nagel, Düren, Germany) according to the manufacturer's instructions. The quality and amount of extracted RNA were estimated using a microvolume spectrophotometer DS-11 (DeNovix, Wilmington, USA). Then, the integrity of extracted total RNAs was assessed using the RNA 6 000 Nano kit (Agilent Technologies France, Massy, France) with the Agilent 2100 Bioanalyzer (Agilent Technologies). All samples met the quality criteria for qPCR analysis. Means of A260/280 and A260/230 ratios were 2.14 ± 0.02 and 1.99 ± 0.16, respectively. RNA integrity numbers were between 9.3 and 10.0.

First-strand cDNA synthesis was performed with 2 μg of total RNA, by using SuperScript IV Vilo with EZDNase kit according to the manufacturer's instructions. (Thermo Fischer Scientific, Carlsbad, USA). Primers were designed from porcine sequences available in Ensembl or NCBI databases using Primer Express® v3.0 software (Thermo Fischer Scientific). Detailed information on the primer sequences (forward and reverse) is provided in Table 2.

For each primer pair, the amplification efficiency (**E**) of qPCR reaction was determined using calibration curves generated with six decreasing concentrations of cDNA from pooled muscle samples (obtained from 25 to 25E−3 ng RNA). Amplification reaction was performed in duplicate in 12.5 μL with 5 ng of reverse-transcribed RNA and both forward and reverse primers (200 nM each) in 1X PCR buffer (Fast SYBR® Green Master Mix, Thermo Fischer Scientific). Amplification reactions and dissociation curves were carried out on a StepOnePlus TM Applied Biosystems real-time PCR system (Thermo Fischer Scientific), and amplification conditions were as follows: 2 min at 50 °C, 20 sec at 95 °C followed by 40 cycles of 3 sec at 95 °C, 30 s at 60 °C. Specificity of the amplification products was checked by dissociation curve analysis. Beta2 microglobulin was identified as the most stable housekeeping genes and was used for normalisation factor (**NF**) calculation. For

Table 1
List of antibodies used for Western blot analysis.

Antibody	Dilution	Reference	Supplier
AMP-activated kinase α(AMPK)	1:2 000	#2793	Cell signalling technology
Atg5	1:1 000	#12994	Cell signalling technology
Beclin 1 (BECN1)	1:1 000	#3738	Cell signalling technology
Microtubule-associated protein 1 light-chain 3β (LC3)	1:1 000	sc-271625	Santa Cruz Biotechnology
Mitochondrial subunit COX IV (COX IV)	1:2 000	#4850	Cell signalling technology
Mitofusin-1 (MFN1)	1:1 000	#14739	Cell signalling technology
Phosphatidylinositol 3-kinase p100 (PI3K)	1:1 000	sc-365404	Santa Cruz Biotechnology
Phospho-AMPKα (Thr172) (PhAMPK)	1:1 000	#2535	Cell signalling technology
Phosphorylated UNC-51-like kinase-1 (Ser757) (PhULK1)	1:1 000	#6888	Cell signalling technology
Sequestosome1 (SQSTM1)	1:1 000	#5114	Cell signalling technology
Translocase of the outer mitochondrial membrane receptor 20 (TOM20)	1:1 000	#2406	Cell signalling technology

Table 2
Primer and probe sequences used for analysis of gene expression by qPCR.

Gene symbol	Accession number[1]	Primer sequence (5′–3′)
BECN1	ENSSSCT00000063037.1	F: TGCAGGTGAGCTTCGTGTGT R: TGTGGCAAGTAATGGAGCTGTAAG
COX1	ENSSSCT00000019670	F: GAATAGTGGGCACTGCCTTGA R: GGGTTCCGGGCTGACCTA
CS	NM214276.1	F: CCTTTCAGACCCCTACTTGTCCT R: CACATCTTTGCCGACTTCCTTC
LC3B	ENSSSCT00000002946.3	F: TGCCGTCCGAGAAAACCTT R: GGATGCTGCTCTCGGATGAG
MyHC emb	XM_003131994.2	P: CTACGCGACCTTCG F: GGCACCGTGGACTACAGTGT R: AGTCGTCCTTAAATTCGACATCAG
MyHC fet	XM_003483113	P: CTACATACGCTAGTGCTGAA F: GGCACCGTGGACTACAGTGT R: TGCTCCTCAGATTGGTCATCAG
ND4	ENSSSCT00000019682.3	F: CCACATGACTCCTCCCCCTTA R: TCGGGTTGTGGTTTCTTTTGA
PAX7	XM_005659088	F: CGGATGTGGAGAAAAAGATTGAG R: CGGATCTCCCAGCTGAACA
PPARGC1a	NM_213963.1	F: CGCAAGCAATTTTTCAAGTCTAAC R: GGAAGCAGGATCAAAGTCATCTG
SQSTM1	ENSSSCT00000015311.3	F: GCAGCCTGAGGAACAGATGG R: GGCCCTTCAGATTCAGGCAT
MYOD	ENSSSCT00000014609	F: GCCGCTTGAGCAAAGTCAA R: CGCTGATTCGGGTTGCTAGA
MYOG	ENSSSCT00000016858	F: CCAGGAACCCCACTTCTATGAC R: GTAGCCTGGTGGCTCAAAGC
B2M[2]	NM_213978	F: GCCATTCCAGTCAGGTTCTACAC R: TCCAATAGAATTCCACACCATGAA

Abbreviations: BECN1, beclin-1; COX1, cytochrome c oxidase subunit 1; mitochondrial; CS, citrate synthase; LC3B, Microtubule-associated protein 1 light-chain 3 beta; MyHC emb, Myosin Heavy Chain Embryonic; MyHC fet, Myosin Heavy Chain perinatal; ND4, NADH-Ubiquinone Oxidoreductase Chain 4; PAX7, PAired boX 7; PPARGC1a, peroxisome proliferator-activated receptor gamma coactivator 1-alpha, mitochondrial; SQSTM1, Sequestosome 1; MYOD, Myogenic differentiation 1; MYOG, Myogenin; B2M, beta2 microglobulin.
[1] Accession number in the National Center for Biotechnology Information (NCBI) and Ensembl project databasis for pig sequences. P, F and R indicated probe, forward and reverse primers, respectively.
[2] Gene used as reference for normalisation.

all examined genes, the normalised expression level **N** was calculated according to the formula developed by Pfaffl (2001): $N = E^{-\Delta Cq(\text{sample-calibrator})}/NF$ where E is calculated from the amplification efficiency, Cq is the quantification cycle, and calibrator is a pool of all samples. For all studied genes, E was between 1.82 and 2.17.

Statistical analyses

For statistical analyses, ANOVA was performed using R software (version 3.5.1). Cell culture time (D0, D1, D3) was considered as fixed effects for autophagy analyses. Cell culture time (D0, D1, D3), bafilomycin treatment and their interaction were considered as fixed effects for autophagic flux analyses. Error bars indicate SD. Differences were considered statistically significant if $P \leq 0.05$ and were discussed as a trend if $0.05 < P < 0.1$.

Results

Myogenic differentiation of pig satellite cells

Immediately after isolation, pig LM muscle satellite cells exposed to high-serum medium rapidly proliferated (3–4 days) in undifferentiated state. However, when exposed to low-serum medium, they started to differentiate at day 1 (D1) and become phase-bright multinucleated fused myotubes (Fig. 1A). The presence of MyHC was assessed by the use of the MF20 monoclonal antibody which reacts with all skeletal MyHC isoforms. At the end of the proliferative phase (D0), very rare mononuclear cells began to express MyHC while at days 1 and 3 (D1 and D3) and the fusion percentage was about 25 and 32% respectively. Western blotting revealed a marked decrease in Paired Box 7 (**PAX7**) expression from day 0 (D0) to D1 and D3 ($P = 0.004$) while MyHC increased ($P = 0.03$) (Fig. 2A). As shown in Fig. 2B, Myogenic Differentiation 1 (**MYOD**) mRNA expression also decreased during cell differentiation ($P = 0.02$). PAX7 and Myogenin (**MYOG**) mRNA expression were not significantly different. Among all MyHC isoforms, only embryonic and foetal MyHC mRNA were expressed in satellite cells and their levels increased during differentiation (Fig. 2C).

Activation of autophagy during differentiation

Molecular protein markers of autophagy initiation, elongation and degradation steps were investigated (Fig. 3). Phosphorylated UNC-51-like kinase-1 (**PhULK1**) and Phosphatidylinositol 3-kinase (**PI3K**), two proteins of the initiation step were markedly decreased during cell differentiation but only PI3K was different ($P = 0.003$) probably due to PhULK variability at the initial point of measurement. Sequestosome 1 (**SQSTM1**) protein level also decreased ($P = 0.01$) (Fig. 3A and B). The level of microtubule-associated protein 1 light-chain 3β (**LC3**I) protein, the most widely monitored autophagy-related protein, was similar in the three investigated days (Fig. 3B) but the amount of LC3II, a processed form of LC3I correlated with the extend of autophagosome formation, increased during differentiation so that LC3II/LC3I ratio increased drastically during muscle satellite cell differentiation ($P < 0.001$) (Fig. 3C). The mRNA expression of Beclin 1 (**BECN1**) and light-chain 3B (**LC3B**) did not differ but the expression of SQSTM1 decreased ($P = 0.005$) (Fig. 3D).

Autophagic flux using bafilomycin

The addition of bafilomycin (**baf**) in cell culture medium 2 h before cells harvesting resulted in the accumulation of LC3II

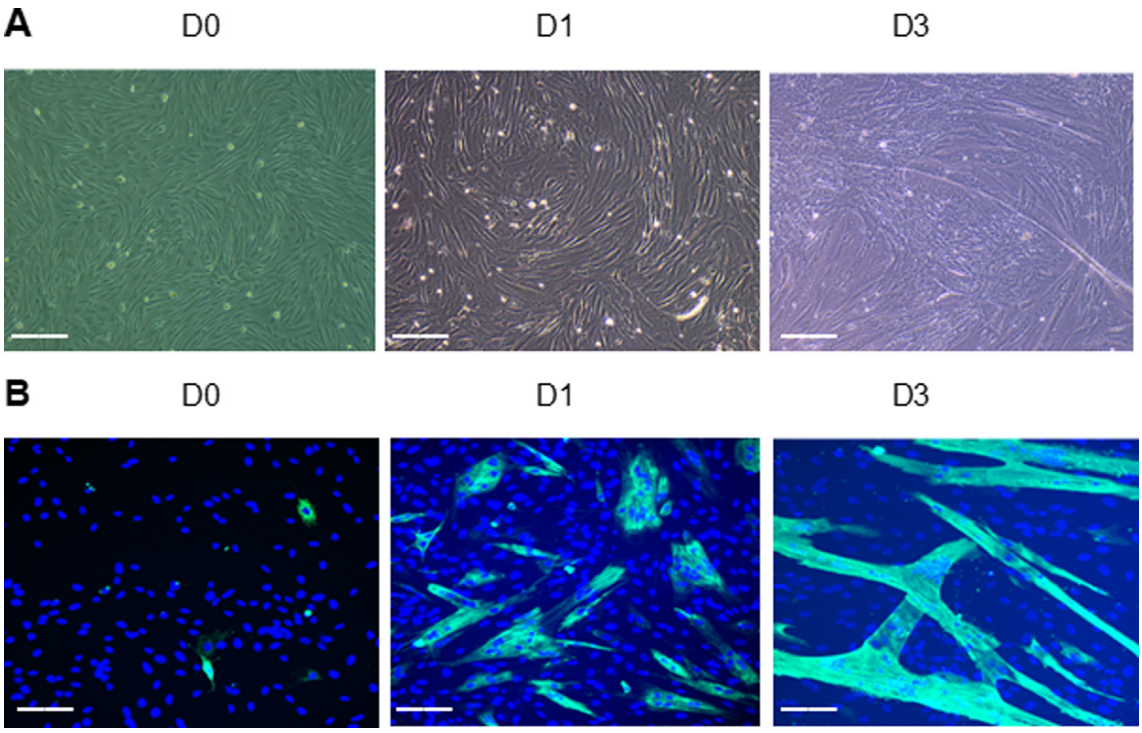

Fig. 1. Myogenic differentiation of piglet satellite cells. Cells were first cultured in proliferating medium until 80% confluence (D0) and switched in differentiation medium during 1 (D1) or 3 days (D3). A: Phase contrast microscopy. Scale bar = 200 μm. B: Cells were immunostained for Myosin Heavy Chain (green) and DAPI (blue) and examined with fluorescence microscopy. Scale bar = 100 μm.

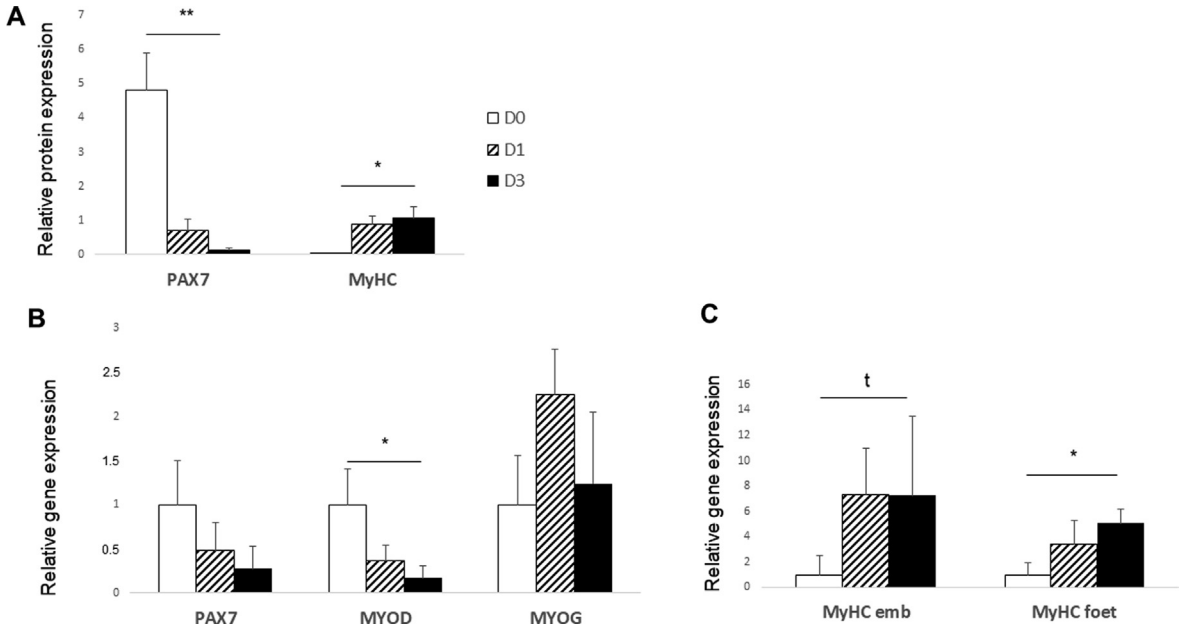

Fig. 2. Molecular markers of piglet satellite cell differentiation. Cells were cultured in proliferating medium until 80% confluence (D0) and switched in differentiation medium during 1 (D1) or 3 days (D3). A: Protein abundance of Paired box protein Pax-7 (PAX7) and Myosin Heavy Chain (MyHC) were measured by Western blot. B, C: Relative gene expression of PAX7, Myoblast determination protein 1 (MYOD), Myogenin (MYOG), embryonic and foetal Myosin Heavy Chain (MyHC emb, MyHC fet) were measured by qPCR. (t $0.05 \leq P < 0.10$, $^{*}P < 0.05$; $^{**}P < 0.01$; $^{***}P < 0.001$).

protein but did not change LC3I protein level when compared to DMSO control treatment. Therefore, LC3II/I protein ratio was increased whatever the day of culture (Fig. 4A) ($P < 0.001$). The phosphorylated APMK (Thr172) protein expression was also stimulated by baf treatment whereas total AMPK protein expression was not modified. Consequently, PhAMPK/AMPK protein ratio was increased ($P = 0.002$) (Fig. 4B).

Energy metabolism is modified during satellite cell differentiation

Relative mitochondrial protein expression of Cytochrome c oxidase subunit IV (**COX IV**), Translocase of the outer mitochondrial membrane receptor 20 (**TOM20**) and Mitofusin-1 (**MFN1**) decreased during the differentiation of satellite cells in culture (Fig. 5A and B). Mitochondrial mRNA expression profiles tended

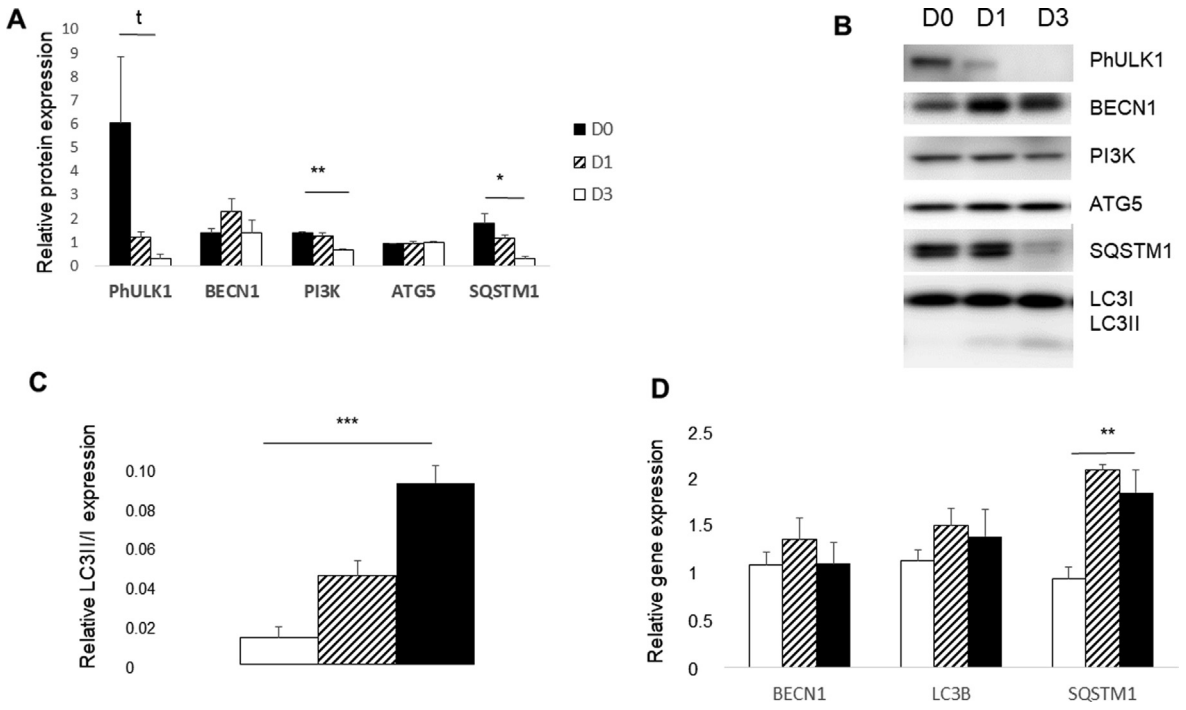

Fig. 3. Piglet satellite cell autophagy during differentiation. Cells were cultured in proliferating medium until 80% confluence (D0) and switched in differentiation medium during 1 (D1) or 3 days (D3). A, B, C: Protein abundance of Phosphorylated UNC-51-like kinase-1 (PhULK1), Beclin 1 (BECN1), Phosphatidylinositol 3-kinase (PI3K), ATG5, Sequestosome 1 (SQSTM1), Microtubule-associated protein 1 light-chain 3β (LC3 I) and LC3II during initiation and elongation step were measured by Western blot. D: Relative gene expression was measured by qPCR. (t $0.05 \leq P < 0.10$, $^{*}P < 0.05$; $^{**}P < 0.01$; $^{***}P < 0.001$).

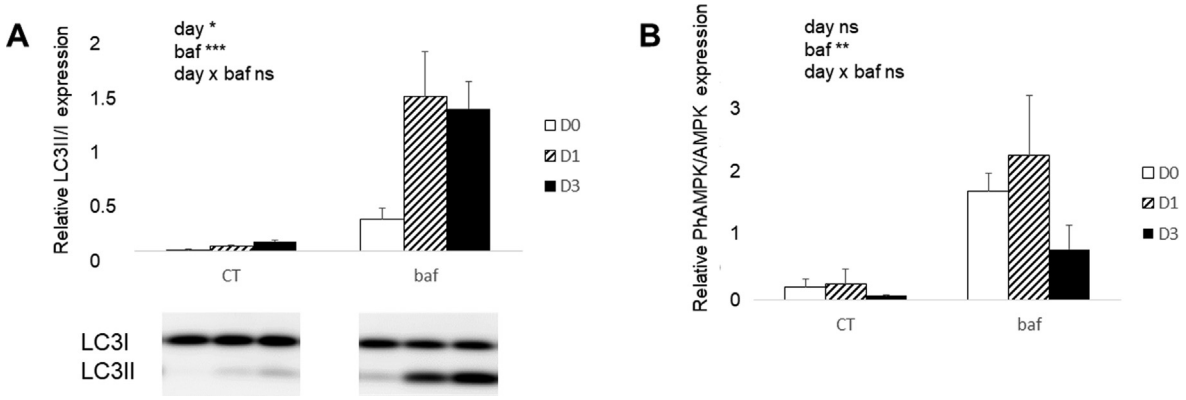

Fig. 4. Autophagic flux measurement during piglet satellite cell differentiation. Cells were cultured in proliferating medium until 80% confluence (D0) and switched in differentiation medium during 1 (D1) or 3 days (D3). Cells were then treated during 2 h with bafilomycin. A, B: protein abundance of the two bands of Microtubule-associated protein 1 light-chain 3β (LC3II/LC3I ratio) and PhAMPK/AMPK were measured by Western blot. CT: control, baf: bafilomycin treatment, ns: not significant.

to decrease for cytochrome c oxidase subunit 1 (**COX1**) and peroxisome proliferator-activated receptor gamma coactivator 1-alpha (**PPARGC1a)** while citrate synthase and NADH-Ubiquinone Oxidoreductase Chain 4 mRNA were not significantly different after differentiation (Fig. 5C).

Author's point of view

In the current study, we successfully identified specific antibodies allowing autophagy key protein quantification and autophagy flux measurements in pig skeletal muscle. We used an *in vitro* cell culture system developed previously in our laboratory (Perruchot et al., 2012) allowing investigations of pig muscle satellite cell in culture. LM muscle satellite cells were obtained from 3- to 4-day-old piglets because satellite cell yield has been shown to decrease with age in pigs (Zhu et al., 2013; Miersch et al., 2017).

The expression of myogenic markers during culture confirmed our satellite cell model ability to proliferate and then to differentiate into myogenic lineage as previously shown in newborn piglets (Mau et al., 2008; Perruchot et al., 2012; Miersch et al., 2018). The observed fusion percentage (32% after 3 days of culture in differentiation medium) supports the good ability of our SC to form multinucleated myotubes when compared with other studies (from 20 to 65%). The MHC transcripts detected in our model are predominantly embryonic forms of the contractile-specific gene assuming immature muscle myofibres in accordance with previous studies in pigs (Zhu et al., 2013; Perruchot et al., 2012). Indeed, we did not detect adult myosin isoforms. However, the expression of myogenic marker genes like PAX7, MYOD and MYOG confirmed the ability of our satellite cells to be activated and to commit differen-

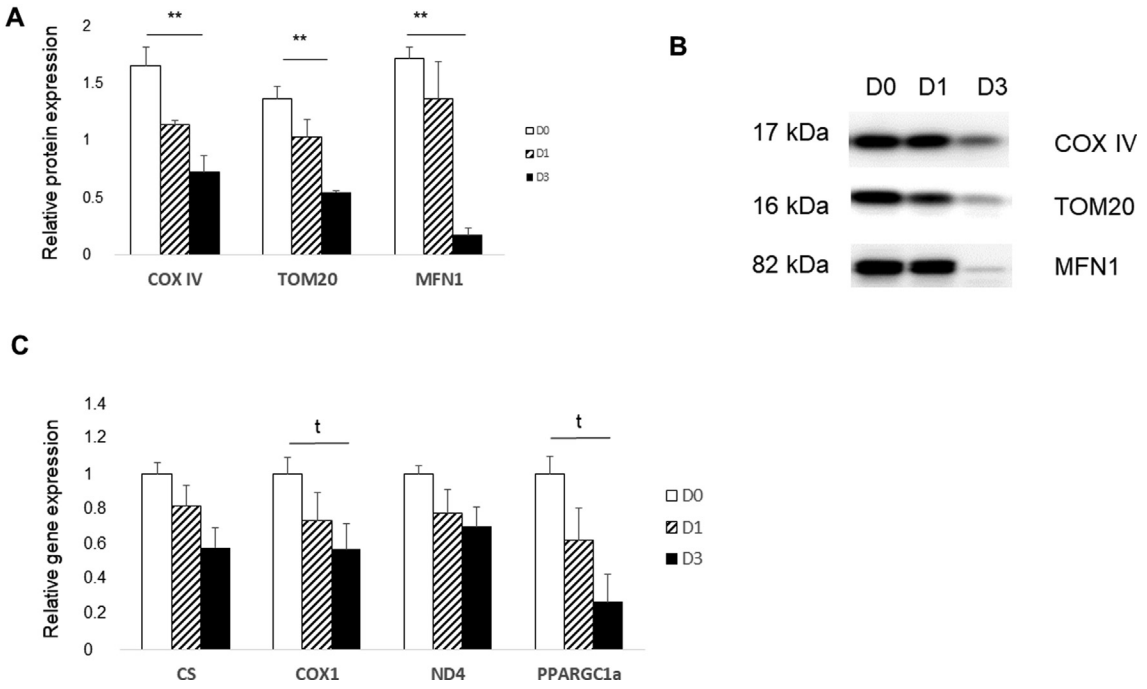

Fig. 5. Piglet satellite cell metabolism during differentiation. Cells were cultured in proliferating medium until 80% confluence (D0) and switched in differentiation medium during 1 (D1) or 3 days (D3). A, B: Protein abundance of Mitochondrial subunit COX IV (COX IV), Translocase of the outer mitochondrial membrane receptor 20 (TOM20) and Mitofusin-1 (MFN1) were measured by Western blot. C: Relative gene expression of citrate synthase (CS), cytochrome c oxidase subunit 1 (COX1), NADH-Ubiquinone Oxidoreductase Chain 4 (ND4) and peroxisome proliferator-activated receptor gamma coactivator 1-alpha (PPARGC1) were measured by qPCR. (t $0.05 \leq P < 0.10$, $^{*}P < 0.05$; $^{**}P < 0.01$; $^{***}P < 0.001$).

tiation. PAX7 and MYOD expression decreased during cell differentiation confirming their loss of stemness status whereas the lack of change in the expression of the terminally committed SC marker MYOG is consistent with non-mature fibre phenotype unlike other findings (Miersch et al., 2017).

In this study, we successfully detected and quantified key autophagy-related proteins in pig muscle satellite cells *in vitro*. We used immunoblotting, a widely used analytical technique for the investigation of microtubule-associated protein LC3B (Mizushima et al., 2010; Klionsky et al., 2012; Yoshii and Mizushima, 2017). Indeed, LC3 is detected as two bands by immunoblotting. The first one, LC3I, the cleaved form of LC3 is present in the cytosol. The other one, named LC3II, is the LC3I form conjugated to phosphatidylethanolamine (**PE**) which is associated with the autophagosome membrane. We observed a rapid increase in LC3II form quickly upon switching cells in the differentiation medium. Consequently, an increased LC3II/LC3I ratio, used as a marker of the number of autophagosomes, confirmed the occurrence of autophagy during myogenesis (Fortini et al., 2016).

To confirm that autophagy is activated, we measured autophagic flux with bafilomycin, which inhibits autophagosome-lysosome fusion and induced autophagosome accumulation confirming ongoing autophagy during satellite cell differentiation (Mizushima and Yoshimori, 2007). With the specific antibodies identified, the following proteins can be quantified: PhULK1, PI3K, BECN1, ATG5 and SQSTM1. Our results confirmed autophagy activation along with satellite cell differentiation. The observation of a decreased levels of PhULK1 and SQSTM1 further supports the induction of autophagy and indicates that SQSTM1 can be used as a marker of autophagic flux. Although immunoblot is the gold method to study autophagy, transcriptional levels of BECN1, LC3B and SQSTM1 were also measured. Only SQSTM1 mRNA level was modified during differentiation. The transcriptional induction of SQSTM1 could be necessary to replenish SQSTM1 protein level. Thus, assessing the mRNA levels of SQSTM1 by qPCR may be relevant for the investigation of autophagy.

As muscle energy metabolism relies highly on mitochondrial oxidative phosphorylation and autophagy plays an important role in the regulation of mitochondrial function (Lee et al., 2011), we investigated mitochondrial population and metabolism. The finding of a reduction of TOM20, COIV and MFN1 protein levels when cells were switched to differentiation media for 3 days is consistent with a decrease in mitochondrial population as shown in C2C12 early myogenic differentiation (Sin et al., 2016). In our model, PPARGC1a and COX1 mRNA levels also tended to be downregulated after 3 days of differentiation confirming mitochondria biogenesis downregulation. In contrast, data obtained in mice support an increase in mitochondrial biogenesis during satellite cell differentiation (Fortini et al., 2016). This discrepancy could be due to our pig non-mature differentiated cell model. In our study, we showed that autophagy inhibition by bafilomycin was associated with an increased PhAMPK/AMPK ratio. AMPK regulates autophagy through direct ULK1 phosphorylation but the exact phosphorylation sites remain unclear (Kim et al., 2011; Laker et al., 2017).

The phosphorylation of AMPK at tyrosine 172 in response to autophagosome and lysosome fusion inhibition after 2 h incubation with bafilomycin confirmed the immediate activation of AMPK as shown by Laker et al. (2017). These authors observed a transient AMPK activation immediately after a single bout of exercise without alteration of mitochondrial fusion protein 2. In the current study, we also did not detect any modifications of MTFN1 and TOM20, two mitochondrial structural proteins. The AMPK response could be an answer of the satellite cells to cellular energy decrease due to blockage of macromolecule release after autophagy inhibition by bafilomycin incubation.

In conclusion, with the use of an in vitro satellite cell model, we validated markers to study autophagy in pig muscle. We further demonstrated the activation of autophagy during satellite cell differentiation. These markers will be useful to better understand the role of autophagy in the development and homeostasis of porcine tissues and cells.

Ethics approval

Not required.

Author ORCIDs

Annie Vincent: https://orcid.org/0000-0002-8140-0799.
Frédéric Dessauge: https://orcid.org/0000-0002-5785-2365.
Isabelle Louveau: https://orcid.org/0000-0001-9684-6294.

Author contributions

A.V. and **F.D.** studied design, performed experiments, data analysis and interpretation. **A.V.** wrote the first draft of the paper and confirmed the final manuscript. **F.D.** and **I.L.** helped to draft the manuscript, read and approved the final version of the manuscript.

Declaration of interest

The authors declare no competing interests.

Acknowledgements

None.

Financial support statement

This research received no specific grant from any funding agency, commercial or not-for-profit section.

References

Biressi, S., Tagliafico, E., Lamorte, G., Monteverde, S., Tenedini, E., Roncaglia, E., Ferrari, S., Cusella-De Angelis, M.G., Tajbakhsh, S., Cossu, G., 2007. Intrinsic phenotypic diversity of embryonic and fetal myoblasts is revealed by genome-wide gene expression analysis on purified cells. Developmental Biology 304, 633–651.
Cheung, T.H., Rando, T.A., 2013. Molecular regulation of stem cell quiescence. Nature Reviews Molecular Cell Biology 14, 329–340.
Danoviz, M.E., Yablonka-Reuveni, Z., 2012. Skeletal muscle satellite cells: background and methods for isolation and analysis in a primary culture system. Methods in Molecular Biology 798, 21–52.
Faure, J., Lefaucheur, L., Bonhomme, N., Ecolan, P., Meteau, K., Coustard, S.M., Kouba, M., Gilbert, H., Lebret, B., 2013. Consequences of divergent selection for residual feed intake in pigs on muscle energy metabolism and meat quality. Meat Science 93, 37–45.
Fortini, P., Ferretti, C., Iorio, E., Cagnin, M., Garribba, L., Pietraforte, D., Falchi, M., Pascucci, B., Baccarini, S., Morani, F., Phadngam, S., De Luca, G., Isidoro, C., Dogliotti, E., 2016. The fine tuning of metabolism, autophagy and differentiation during in vitro myogenesis. Cell Death and Disease 7, e2168–e.
Kim, J., Kundu, M., Viollet, B., Guan, K.-L., 2011. AMPK and mTOR regulate autophagy through direct phosphorylation of Ulk1. Nature Cell Biology 13, 132–141.
Klionsky, D.J., Abdelmohsen, K., Abe, A., Abedin, M.J., Abeliovich, H., Acevedo Arozena, A., Adachi, H., Adams, C.M., Adams, P.D., Adeli, K., et al., 2012. Guidelines for the use and interpretation of assays for monitoring autophagy. Autophagy 12, 1–222.
Laker, R.C., Drake, J.C., Wilson, R.J., Lira, V.A., Lewellen, B.M., Ryall, K.A., Fisher, C.C., Zhang, M., Saucerman, J.J., Goodyear, L.J., Kundu, M., Yan, Z., 2017. Ampk phosphorylation of Ulk1 is required for targeting of mitochondria to lysosomes in exercise-induced mitophagy. Nature Communication 8, 548.
Lee, J., Giordano, S., Zhang, J., 2011. Autophagy, mitochondria and oxidative stress: cross-talk and redox signaling. Biochemical Journal 441, 523–540.
Masiero, E., Agatea, L., Mammucari, C., Blaauw, B., Loro, E., Komatsu, M., Metzger, D., Reggiani, C., Schiaffino, S., Sandri, M., 2009. Autophagy is required to maintain muscle mass. Cell Metabolism 10, 507–515.
Mau, M., Oksbjerg, N., Rehfeldt, C., 2008. Establishment and conditions for growth and differentiation of a myoblast cell line derived from the semimembranosus muscle of newborn piglets. In Vitro Cellular and Developmental Biology Animal 44, 1–5.
Miersch, C., Stange, K., Hering, S., Kolisek, M., Viergutz, T., Röntgen, M., 2017. Molecular and functional heterogeneity of early postnatal porcine satellite cell populations is associated with bioenergetic profile. Scientific Reports 7, 45052.
Miersch, C., Stange, K., Röntgen, M., 2018. Separation of functionally divergent muscle precursor cell populations from porcine juvenile muscles by discontinuous Percoll density gradient centrifugation. BMC Molecular and Cell Biology 19, 2.
Mizushima, N., 2007. Autophagy: process and function. Genes and Development 21, 2861–2873.
Mizushima, N., Yoshimori, T., 2007. How to interpret LC3 immunoblotting. Autophagy 3, 542–545.
Mizushima, N., Yoshimori, T., Levine, B., 2010. Methods in mammalian autophagy research. Cell 140, 313–326.
Montarras, D., L'honoré, A., Buckingham, M., 2013. Lying low but ready for action: the quiescent muscle satellite cell. FEBS Journal 280, 4036–4050.
Perrotta, C., Cattaneo, M.G., Molteni, R., De Palma, C., 2020. Autophagy in the regulation of tissue differentiation and homeostasis. Frontiers in Cell and Developmental Biology 8, 1563.
Perruchot, M.-H., Ecolan, P., Sorensen, I.L., Oksbjerg, N., Lefaucheur, L., 2012. *In vitro* characterization of proliferation and differentiation of pig satellite cells. Differentiation 84, 322–329.
Pfaffl, M.W., 2001. A new mathematical model for relative quantification in real-time RT-PCR. Nucleic Acids Research 29, e45.
Relaix, F., Bencze, M., Borok, M.J., Der Vartanian, A., Gattazzo, F., Mademtzoglou, D., Perez-Diaz, S., Prola, A., Reyes-Fernandez, P.C., Rotini, A., Taglietti, T., 2021. Nature Communication 12, 692.
Rubio-González, A., Potes, Y., Illán-Rodríguez, D., Vega-Naredo, I., Sierra, V., Caballero, B., Fàbrega, E., Velarde, A., Dalmau, A., Oliván, M., Coto-Montes, A., 2015. Effect of animal mixing as a stressor on biomarkers of autophagy and oxidative stress during pig muscle maturation. Animal 9, 1188–1194.
Schneider, C.A., Rasband, W.S., Eliceiri, K.W., 2012. NIH Image to ImageJ: 25 years of image analysis. Nature Methods 9, 671–675.
Sin, J., Andres, A.M., Taylor, D.J.R., Weston, T., Hiraumi, Y., Stotland, A., Kim, B.J., Huang, C., Doran, K.S., Gottlieb, R.A., 2016. Mitophagy is required for mitochondrial biogenesis and myogenic differentiation of C2C12 myoblasts. Autophagy 12, 369–380.
Suryawan, A., Davis, T.A., 2014. Regulation of protein degradation pathways by amino acids and insulin in skeletal muscle of neonatal pigs. Journal of Animal Science and Biotechnology 5, 8.
Tang, A.H., Rando, T.A., 2014. Induction of autophagy supports the bioenergetic demands of quiescent muscle stem cell activation. Journal of the European Molecular Biology Organization 33, 2782–2797.
Tesseraud, S., Avril, P., Bonnet, M., Bonnieu, A., Cassar-Malek, I., Chabi, B., Dessauge, F., Gabillard, J.-C., Perruchot, M.-H., Seiliez, I., 2021. Autophagy in farm animals: current knowledge and future challenges. Autophagy 17, 1809–1827.
Theil, P.K., Sorensen, I.L., Nissen, P.M., Oksbjerg, N., 2006. Temporal expression of growth factor genes of primary porcine satellite cells during myogenesis. Animal Science Journal 77, 330–337.
Vincent, A., Perruchot, M.H., Louveau, I., Dessauge, F., 2020. Autophagy is required for in vitro myogenesis in piglets. Book of abstracts of the 71st annual meeting of the European Federation of Animal Science, 1–4 December 2020, virtual meeting, pp 354.
Yoshii, S.R., Mizushima, N., 2017. Monitoring and Measuring Autophagy. International Journal of Molecular Sciences 18, 1865.
Zecchini, S., Giovarelli, M., Perrotta, C., Morisi, F., Touvier, T., Di Renzo, I., Moscheni, C., Bassi, M.T., Cervia, D., Sandri, M., Clementi, E., De Palma, C., 2018. Autophagy controls neonatal myogenesis by regulating the GH-IGF1 system through a NFE2L2- and DDIT3-mediated mechanism. Autophagy 15, 58–77.
Zhu, H., Park, S., Scheffler, J.M., Kuang, S., Grant, A.L., Gerrard, D.E., 2013. Porcine satellite cells are restricted to a phenotype resembling their muscle origin. Journal of Animal Science 91, 4684–4691.